HHS Public Access

Author manuscript

Nat Biotechnol. Author manuscript; available in PMC 2019 May 19.

RNAi Modulation of Placental sFLT1 for the Treatment of Preeclampsia.

Anton A. Turanov[#1], **Agnes Lo**[#2,3], **Matthew R. Hassler**[#1], **Angela Makris**[#4,5,6], **Ami Ashar-Patel**[1], **Julia F. Alterman**[1], **Andrew H. Coles**[1], **Reka A. Haraszti**[1], **Loic Roux**[1], **Bruno MDC Godinho**[1], **Dimas Echeverria**[1], **Suzanne Pears**[4], **Jim Iliopoulos**[5], **Renuka Shanmugalingam**[4,5,6], **Robert Ogle**[7], **Zsuzsanna K. Zsengeller**[2,3], **Annemarie Hennessy**[4,5], **S. Ananth Karumanchi**[2,3,8], **Melissa J. Moore**[1,9], and **Anastasia Khvorova**[1,10]

[1]RNA Therapeutics Institute, University of Massachusetts Medical School, Worcester, Massachusetts

[2]Center for Vascular Biology Research, Beth Israel Deaconess Medical Center

[3]Harvard Medical School, Boston, Massachusetts

[4]Heart Research Institute, Sydney

[5]School of Medicine, Western Sydney University, Sydney

[6]Renal Department, Liverpool Hospital, Sydney

[7]Women's and Babies, Royal Prince Alfred Hospital, Sydney

[8]Deparment of Medicine, Cedars-Sinai Medical Center, Los Angeles, California

[9]Moderna Therapeutics, Cambridge, Massachusetts

[10]Program in Molecular Medicine, University of Massachusetts Medical School, Worcester, Massachusetts

[#] These authors contributed equally to this work.

Abstract

Preeclampsia (PE) is a placentally-induced hypertensive disorder of pregnancy that is associated with significant morbidity and mortality to mothers and fetuses. Clinical manifestations of preterm PE result from excess circulating soluble vascular endothelial growth factor receptor FLT1 (sFLT1

Author contributions

A.A.T. managed the project, performed most of the experiments, and drafted the manuscript. M.J.M., S.A.K., and A.K. conceptualized the study and led the project. M.R.H., D.E. and L.R. synthesized all compounds, and developed and optimized protocols for gram-scale synthesis. A.H.C. and B.MDC.G. helped with in vivo studies. R.A.H. performed PNA assay analysis. A.A-P. performed PAS-seq analysis and an initial siRNA screen. J.F.A. helped with the siRNA screen. A.L. performed primary cytotrophoblast isolations, ELISAs, toxicity studies and mouse pregnancy studies. Z.K.Z. performed placenta vascular immunohistochemistry. A.H., A.M., S.P., J.I., R.S., R.O. developed the baboon PE model and performed all baboon experiments. A.A.T, A.K., M.J.M., S.A.K., and A.H. wrote the manuscript.

Conflict of interest

A.K. discloses ownership of stock in RXi Pharmaceuticals and Advirna. S.A.K. is a consultant to Thermofisher Scientific and owns stock in Aggamin Therapeutics. Other authors declare no conflict of interest.

or sVEGFR1) of placental origin. Here we identify short interfering RNAs (siRNAs) that selectively silence the three *sFLT1* mRNA isoforms primarily responsible for placental overexpression of sFLT1. Full chemical stabilization in the context of hydrophobic modifications enables productive siRNA accumulation in the placenta (up to 7% of injected dose) and reduces circulating sFLT1 in pregnant mice (up to 50%). In a baboon PE model, single dose of siRNAs suppressed sFLT1 overexpression and clinical signs of PE. Our results demonstrate RNAi-based extra-hepatic modulation of gene expression with non-formulated siRNAs in non-human primates and establish a path toward a new treatment paradigm for patients with preterm PE.

Preeclampsia (PE) complicates 5%–10% of all human pregnancies, and causes nearly 76,000 maternal and 500,000 infant deaths globally each year. In the United States alone, PE is responsible for 100,000 premature births and 10,500 infant deaths annually, with aggregated costs of ~6.5-billion dollars to the health care system[1] (www.preeclampsia.org). Preeclamptic women rapidly develop hypertension often with proteinuria, usually after the 20th week of pregnancy. Maternal complications include kidney injury, HELLP (hemolysis, elevated liver enzymes, and low platelets) syndrome, seizure, stroke, and death. Consequences for the fetus can be grave, ranging from intra-uterine growth restriction to hypoxia-induced neurologic injury (e.g., cerebral palsy) to death. Currently the only treatment option for women with PE is to deliver the fetus—regardless of its gestational age—when the mother's symptoms become too severe. Thus, PE represents a significant public health concern with an unmet clinical need.

Epidemiological and experimental studies indicate that the maternal signs and symptoms of PE that presents preterm are caused by abnormally high serum levels of soluble fms-like tyrosine kinase 1 (sFLT1) proteins[2–10]—secreted anti-angiogenic proteins that correspond to the extracellular domain of vascular endothelial growth factor receptor 1 (VEGFR1; aka full length FLT1). sFLT1 proteins scavenge circulating VEGF and placental growth factor, and attenuate VEGF signaling by membrane-bound VEGF receptor FLT1[11,12]. Circulating sFLT1 levels rapidly decrease after delivery of the placenta, and maternal PE symptoms usually resolve within 48 to 72 hours, consistent with the placental origin of sFLT1[2, 13]. Serum sFLT1 levels are considered a diagnostic and prognostic marker of PE[14–17]. Moreover, lowering sFLT1 and other circulating factors by apheresis—i.e., filtering maternal blood through a dextran sulfate column—can control both blood pressure and proteinuria and extend PE pregnancies[18,19]. Thus, sFLT1 is a biologically validated and clinically promising therapeutic target for PE.

Short interfering RNA (siRNA) therapeutics is an emerging class of drugs that target nucleic acids[20]. The most clinically advanced siRNA technology comprises fully chemically stabilized siRNAs conjugated to N-acetyl galactosamine (GalNAc), which drives safe, efficient siRNA delivery to and long-lasting (6- to 9-month) silencing activity in liver[21,22]. Whereas the utility of GalNAc chemistry is limited to hepatocytes, hydrophobic conjugates (e.g., cholesterol) enable non-selective siRNA distribution to a range of tissues[23, 24,25, 26], favoring tissues with high blood flow and fenestrated endothelium. These tissue characteristics are shared by the placenta, suggesting that fully chemically modified,

cholesterol-conjugated siRNAs[23, 24, 26, 27] might also accumulate in placenta and allow selective silencing of sFLT1.

As a first step toward developing siRNAs that selectively silence sFLT1 but not full-length FLT1, we recently analyzed the transcriptional profiles and 3' ends of *sFLT1* and *FLT1* mRNAs in normal and preeclamptic placentas[28]. *sFLT1* and *FLT1* mRNAs are predominantly expressed in the placenta, with *sFLT1* mRNA isoforms comprising as much as 97% of placental *FLT1* mRNAs. Use of alternative polyadenylation sites in intron 13 and exon 15 give rise to three dominant *sFLT1* mRNA isoforms—*sFLT1-i13* short, *sFLT1-i13* long, and *sFLT1-e15a* (Fig. 1a,b), which all are upregulated in preeclamptic placentas[28] (Supplementary Fig. 1). The unique 3' ends of the *sFLT1* isoforms offer an opportunity to selectively target *sFLT1.*

Here we identify siRNAs that selectively silence *sFLT1* mRNA without affecting full-length *FLT1.* Full chemical stabilization and cholesterol conjugation allow systemically delivered siRNAs to accumulate in mouse and baboon placentas, where they silence *sFLT1* mRNA. Finally, we show that *sFLT1*-targeting siRNAs lower circulating sFLT1 protein levels and alleviate hypertension and proteinuria in a baboon model of PE. Taken together, these results provide a strong foundation for future development of an siRNA-based therapeutic for PE.

Results

Screen to identify siRNAs selectively silencing i13 and e15 *sFLT1* mRNA isoforms.

Three *sFLT1* mRNA isoforms, *sFLT1-i13* short, *sFLT1-i13 long*, and *sFLT1-e15a* predominantly contribute to the expression of sFLT1 protein, that circulates at high levels in patients with preterm PE[4, 28–30]. Thus all three isoforms need to be targeted to productively decrease the levels of circulating sFLT1 protein across the spectrum of PE patients. The *sFLT1-i13* long and *sFLT1-e15a* mRNA isoforms contain 435 and 567 unique nucleotides, respectively, not present in full-length *FLT1* mRNA, allowing selective targeting. We designed a panel 26 siRNAs targeting essentially all possible regions in both *sFLT-i13* isoforms (*sFLT1-i13*-long includes the *sFLT1-i13*-short sequence) and 21 siRNAs targeting *sFLT1-e15a*. The selection was favored, to the extent possible, to comply with conventional siRNA design parameters[31] that account for GC content, specificity and low frequency of complementary seed sites in the genome[32], and thermodynamic bias[33, 34]. Design criteria also favored siRNAs that target sites with perfect homology in non-human primates, to enable evaluation in a baboon PE model (see below).

For initial *in vitro* screening, we synthesized hydrophobically modified asymmetric siRNAs (hsiRNAs), which can be added directly to the cell medium—e.g., without lipid formulation. hsiRNAs are partially chemically modified for improved stability, and composed of a 20-nucleotide (nt) guide strand base paired to a 15-nt passenger strand, leaving a fully phosphorothioate-modified single-stranded tail at the 3' end of the guide strand[23, 25, 35–37]. The phosphorothioated tail containing siRNAs were more potent in cellular uptake and *sFLT1* silencing compare to fully duplexed (symmetrical) siRNAs[27]. The 3' end of the passenger strand is conjugated to cholesterol, which promotes membrane intercalation and rapid, efficient internalization by all cell types[37, 38], including primary trophoblasts. All

sequences and chemical modification patterns used in this study are shown in Supplementary Table 1.

To simplify the screening process, we generated luciferase-based reporters in which the *sFLT1-i13* and *sFLT1-e15a* unique sequence regions were cloned downstream of the *Renilla* luciferase coding region. We then assayed the ability of each hsiRNA to reduce *Renilla* luciferase activity as a proxy for productive silencing of *sFLT1-i13* and *sFLT1-e15a*. Primary screens identified several functional hsiRNAs that efficiently silence *sFLT1-i13* or *sFLT1-e15a* mRNA isoforms. (Fig. 1c,d;see *Methods* for details). Based on dose-response studies of all functional hsiRNAs, we chose the top two hsiRNAs from each primary screen as lead configurations: hsiRNA^{sFLT1}-2283 and hsiRNA^{sFLT1}-2318 for silencing of *sFLT1-i13*, and hsiRNA^{sFLT1}-2519 and hsiRNA^{sFLT1}-2585 for silencing *sFLT1-e15a*. The half-maximal inhibitory concentrations (IC50) of selected compounds ranged from 50 to 90 nM (passive uptake), and their sequences and target positions are shown at Figure 1e,f,g.

To confirm that lead hsiRNAs efficiently silence *sFLT1* mRNAs in a cell type relevant to PE, we used QuantiGene® 2.0 assays that allow specific and direct detection of human *sFLT1-i13* and *sFLT1-e15a* mRNAs in human primary cytotrophoblasts (CTB), the placental cell type responsible for sFLT1 overexpression. Identified hsiRNAs silenced *sFLT1* mRNAs in cytotrophoblasts, with IC50 values comparable to those found in the reporter assay (50 to 70nM; Fig. 1e,h,i). Moreover, productive silencing of *sFLT1* mRNA translated to a significant reduction in the amount of sFLT1 protein secreted by cytotrophoblasts into the cell media (Fig. 1j). hsiRNA$^{sFLT1\text{-}i13}$-2283 target sequences are conserved in human, baboons, and mouse; hsiRNA$^{sFLT1\text{-}e15a}$-2519 target sequences are conserved in baboons and humans. We therefore selected these compounds for all subsequent studies.

hsiRNA$^{sFLT1\text{-}i13}$-2283 and siRNA$^{sFLT1\text{-}e15a}$-2519 efficiently modulate expression of major *sFLT1* mRNA isoforms without effect on full length *FLT1* mRNA.

Successful therapeutic reduction of circulating sFLT1 in PE using hsiRNAs will require simultaneous suppression of all three *sFLT1* (i13 short and long, and e15a) mRNA isoforms (Fig. 1a,b; Supplementary Fig. 1). We therefore tested whether a mixture of isoform-specific hsiRNAs could be used to silence *sFLT1-i13* and *sFLT1-e15a* mRNAs simultaneously. Using CTB and WM-115 cells (human melanoma cells that express *sFLT1-i13* and *sFLT1-e15a* mRNAs), we confirmed that hsiRNA^{sFLT1}-2283 specifically silenced the *sFLT1-i13* isoform, and hsiRNA^{sFLT1}-2519 specifically silenced the *sFLT1-e15a* isoform (Fig. 2a,b; Supplementary Fig. 2). An equimolar mixture hsiRNA^{sFLT1}-2283/2519 efficiently silenced both *sFLT1-i13* and *sFLT1-e15a* isoforms (Fig. 2a,b). Neither the individual hsiRNAs nor the hsiRNA mixture affected the levels of full-length *FLT1* mRNA (Fig. 2c). Interestingly, the hsiRNA^{sFLT1}-2283/2519 mixture was more potent than individual hsiRNAs, with the effect being more pronounced for the *sFLT1-i13* isoform. We have confirmed this phenomenon in several independent experiments, and are actively exploring the molecular mechanism.

Efficient *in vivo* delivery of fully chemically modified cholesterol-conjugated hsiRNA^{sFLT1}-2283 to the placental labyrinth by systemic administration.

Productive systemic delivery of non-formulated hsiRNA to placenta had not been previously demonstrated. Although the partially modified siRNAs used for original screening could be taken up by cytotrophoblasts *in vitro*, they failed to accumulate to significant levels in placenta after systemic administration (Supplementary Fig. 3). We recently showed, however, that full chemical stabilization is essential for systemic, conjugate-mediated siRNA delivery[27]. We therefore synthesized fully chemically modified variants of lead compounds, in which all sugars were modified using an alternating 2′-fluoro and 2′-*O*-methyl modification pattern[39]. In addition, all 5'- and 3'-terminal linkages were phosphorothioate-modified, providing additional protection against exonucleases (Fig. 3a). To visualize the extent of delivery to tissues *in vivo*, the passenger strand of hsiRNA^{sFLT1} –2283 was labeled with Cy3 fluorescent dye.

We injected Cy3-labeled hsiRNA^{sFLT1}-2283 into pregnant mice at gestational day 15, harvested tissues twenty-four hours after injection, and examined the tissue distribution of labeled hsiRNA by fluorescence microscopy. hsiRNA^{sFLT1}-2283 mainly accumulated in liver, kidneys, spleen, and placental labyrinth (Fig. 3b), consistent with their high degree of endothelial fenestration and blood flow. The placental labyrinth functions as a maternal–placental barrier and the site of nutrient transport between the maternal and fetal blood (Fig. 3b). Consistent with the barrier function of the labyrinth, Cy3-labeled hsiRNA^{sFLT1}-2283 was detected only in placenta (Fig. 3c). The labyrinth constitutes most of the placental disk, where fetal capillaries are supported by connective tissue and surrounded by trophoblast cells— mononuclear sinusoidal trophoblast giant cells and two layers of multinucleated syncytiotrophoblast cells. Notably, we observed efficient delivery of Cy3-labeled hsiRNA^{sFLT1}-2283 to the placental labyrinth, with no detectable uptake by other cell types in the decidua, the uterine endometrium that forms the maternal part of the placenta. Histological examination showed no obvious pathology associated with oligonucleotide delivery.

To quantify the accumulation of hsiRNA in placenta and other tissues, we used a recently developed PNA-based hybridization assay to directly measure guide strand levels[23, 36]. Consistent with histological examination, fully chemically stabilized, cholesterol-conjugated hsiRNAs accumulated in maternal liver (~200 ng/mg), kidney (~50 ng/mg), spleen (~50 ng/mg), and placenta (10 to 20 ng/mg), but not in other fetal tissues (<0.05 ng/mg, detection limit) (Fig. 3d,e). Notably, placental accumulation of hsiRNA was similar whether administered by subcutaneous (SC) or intravenous (IV) injection (Fig. 3b,d,e). As much as seven percent of injected hsiRNA^{sFLT1}-2283 accumulated in placentas, and the concentration of hsiRNA in the concentration of hsiRNA in placenta was ~20 ng/mg, which was sufficient to induce productive silencing (Fig. 3d-e).

In vivo silencing of placental-derived sFLT1 does not affect pup survival or ability to thrive.

Mice only express the *sFlt1-i13* isoform[40]. Thus, hsiRNA^{sFLT1}-2283, which selectively silences *sFlt1-i13*, was used to test if placental accumulation of hsiRNA results in productive sFLT1-i13 silencing. We injected 20 mg/kg hsiRNA^{sFLT1}-2283 in phosphate buffered saline

(PBS) intravenously into pregnant mice at gestational days 14 and 15 (Fig. 4a). Control animals were treated with PBS or, a non-targeting control (NTC) hsiRNA^{NTC} of identical chemical configuration (conjugated to cholesterol and has 2'-O-methyl, 2'-fluoro alternating modification pattern or hsiRNA^{sFLT1}-2283 lacking the cholesterol conjugate (NoC-siRNA^{sFLT1}-2283), (Supplementary Table 1). At gestational day 19, we measured *sFlt1* mRNA levels in placenta. We observed a ~40% reduction of *sFlt1* mRNA in placentas of mice treated with hsiRNA^{sFLT1}-2283 ($P<0.001$, one-way ANOVA, relative to both PBS and hsiRNA^{NTC}, Fig. 4b). The hsiRNA^{NTC} was inactive, showing that *sFlt1* silencing is specific to hsiRNA^{sFLT1}-2283. NoC-siRNA^{sFLT1}-2283 failed to accumulate in placenta (Fig. 4c) and consequently failed to silence *sFlt1* mRNA (Fig. 4b), suggesting that full chemical stabilization and the cholesterol moiety are both required for placental delivery and silencing activity. We found no evidence for silencing of *sFlt1* in fetal liver (data not shown), consistent with the histological and quantitative observations that hsiRNA^{sFLT1}-2283 does not accumulate in fetal tissues other than placenta (Fig. 3c,d,e).

Consistent with significant accumulation of hsiRNA^{sFLT1}-2283 in liver and kidney (Fig. 3d,e), we also observed productive silencing of *sFlt1* mRNA in both of these tissues (Supplementary Fig. 4). In pregnant mice, however, >95% of circulating sFlt1 protein originates from placenta[40–42]. Thus, extra-placental silencing does not measurably contribute to reduced serum levels of sFlt1 in mice treated with hsiRNA^{sFLT1}-2283.

In a parallel study, we treated pregnant mice (at gestational days 14 and 15) with hsiRNA^{sFLT1}-2283, and PBS, and collected blood samples at 3 time points during 3rd trimester to measure serum levels of sFlt1 protein by ELISA. In PBS-treated control mice, sFlt1 protein levels increased by about ~50% from day 14 to day 17 (near term). As expected, this increase was suppressed in mice treated with hsiRNA^{sFLT1}-2283 (Fig. 4d) as evidenced by blood sampling at gestational day 10, 15, 17, and 19 from mice injected with PBS or hsiRNA^{sFLT1}-2283. At each time point, mice treated with hsiRNA^{sFLT1}-2283 expressed lower levels of circulating sFlt1 than did mice treated with PBS ($P<0.001$, two-way ANOVA; Fig. 4d,j) or hsiRNA^{NTC} ($P<0.05$, two-way ANOVA; Fig. 4j). Silencing of *sFlt1* (upto 50%) or treating mice with hsiRNA^{NTC} did not affect the number of newborn pups, their weight at birth, or their ability to thrive (Supplementary Fig. 5a-e). Moreover, the levels of the maternal liver transaminases ALT and AST were normal (Fig. 4e), indicating that at the doses tested, hsiRNA^{sFLT1}-2283 treatment does not generate obvious adverse effects.

To confirm observed modulation of *sFLT1* expression is indeed due to RNAi-based cleavage of *sFlt1* mRNA, we purified total mRNA from placentas treated with hsiRNA^{sFLT1}-2283, hsiRNA^{NTC} and PBS. The purified RNA was subjected to 5'-RACE-PCR amplification. The expected product size was observed only in hsiRNA^{sFLT1}-2283-treated samples and sequencing confirmed the expected cleavage site (Supplementary Fig. 6).

Taken together, these data show that systemic administration of hsiRNA^{sFLT1}-2283 leads to efficient RNAi-based silencing of *sFlt1* mRNA in the placenta and reduces the level of circulating sFlt1 protein without affecting the health of the mother or her pups.

hsiRNA^{sFLT1}-2283/2519 mixture selectively silences *sFLT1-i13* and *-e15a* isoforms *in vivo*.

Our goals were to test whether the mixture of isoform-specific siRNAs effectively silences all three *sFLT1* isoforms in a well characterized non-human primate model of PE[43]. Before doing so, we measured the efficacy and safety of the hsiRNA^{sFLT1}-2283/2519 mixture in pregnant mice. An equimolar mixture of hsiRNA^{sFLT1}-2283/2519 injected into pregnant mice efficiently reduced *sFlt1* mRNA in placenta (40%, $P<0.01$, one-way ANOVA) and other maternal tissues (Fig. 4f). Both hsiRNA^{sFLT1}-2283 and hsiRNA^{sFLT1}-2519 accumulated to nearly identical levels in the placenta, with no detectable transfer to the fetus (Fig. 4g). hsiRNA^{sFLT1}-2283/2519 administration reduced circulating sFlt1 protein levels by day 17 ($P<0.001$, two-way ANOVA), did not affect pup viability, weight, or ability to thrive (data not shown), and maternal liver enzymes remained normal (Fig. 4h,i). The observed reduction in *sFlt1* was sequence specific as hsiRNA^{NTC}, compound with identical chemical configuration, but not targeting *sFlt1* had no impact on *sFlt1* protein expression and was indistinguishable from PBS (Fig. 4j) and had no observable effect on liver enzymes (Fig. 4k). As expected, hsiRNA^{NTC} therapy had no impact on pubs number or ability to strive (Supplementary Fig. 5d,e), confirming that this chemical scaffold was well tolerated at dose used.

While vast majority of sFLT1 expression is placenta derived, sFLT1 is involved in fine-tune regulation of VEGF signaling, specifically important for macular and corneal vascularisation[44, 45]. As shown in Supplementary Figure 7, we do not find any significant levels of the drug in the eye and unlikely to have any biological consequences.

We have not seen any detectable levels of compound transfer to any additional fetal tissues by fluorescent microscopy (Fig. 3c) and PNA hybridization assay (Fig. 3d,e). Breast is another heavily vascularised tissue, in which hydrophobic siRNAs may accumulate. We observed around 2.5 ng/mg of hsiRNA^{sFLT1} compounds in breast tissue of nursing mice after hsiRNA treatment. This compound concentration was more than fivefold lower than levels delivered to placenta of the same animals. No significant compound transfer was observed in milk (< 1ng/μl), indicating that chances for significant fetal hsiRNA accumulation in the fetus via breast milk is minimal (Supplementary Fig. 7).

Although our studies were not designed to formally evaluate pharmacokinetics, in our limited data set, we were unable to detect significant concentrations of the drug in breast tissue or in milk. This in contrast to the robust levels of drug in the placental tissue. Additional pharmacokinetic studies in non-human primates are needed, before we can conclude the low risk for our therapeutic agent to be excreted in breast milk.

Finally, 40 to 50% sFLT1 repression in placenta might have an impact on placenta vascularisation. In a subset of mice injected with the hsiRNA^{sFLT1}, we examined the placental tissue for vascular development and do not find any significant vascular disruptions in the placental labyrinth (Supplementary Fig. 8)[46]. We can therefore conclude that injection of sFlt1 siRNA therapeutic when injected during 3rd trimester and at modest doses does not induce any significant vascular anomalies in the placenta. Although our studies do not show any obvious side effects in mothers or the fetuses, additional long-term safety studies will be needed before drawing definitive conclusion of the safety of this approach.

Thus, co-delivery of hsiRNA^{sFLT1}-2283 and hsiRNA^{sFLT1}-2519 efficiently and safely reduced *sFlt1* without affecting full-length *Flt1* levels, recapitulating the pharmacological behavior observed with hsiRNA^{sFLT1}-2283 alone.

Single hsiRNA^{sFLT1}-2283/2519 injection efficiently modulates sFLT1 serum levels and reduces hypertension and proteinuria in a baboon model of PE.

Placental morphology and physiology differ between humans and mice, limiting the value of rodent models in mimicking human pathology. Placental morphology, maternal physiology, gestation length, and the immune system of baboons (*Papio hamadryas*), however, better resemble those of humans. *P. hamadryas* express all three *sFLT1* mRNA isoforms, and an accepted PE model has been developed[43]. Thus, baboons represent a more accurate pre-clinical model in which to study efficacy, safety, and toxicity of PE therapeutics. Induction of uteroplacental ischemia (UPI) in baboons via ligation of a single uterine artery at gestational day 133 (full term is 182 days) reduces placental blood flow by ~30%, causing a spike in sFLT1 levels and maternal hypertension and proteinuria, typical clinical manifestations of PE[43]. Continuous telemetry recordings accurately measure blood pressure throughout the experiment, allowing real-time assessment of even subtle changes to this key metric.

To assess the potential therapeutic benefit of the hsiRNA^{sFLT1}-2283/2519 mixture in the baboon UPI model of PE, we manufactured and purified ~4 grams of hsiRNA^{sFLT1}-2283/2519 in-house, and then confirmed its identity and purity by mass spectrometry. Working under approved animal safety protocols, we performed the following regimen. On gestational day 127, a telemeter was inserted into a pregnant baboon to continuously monitor blood pressure. On gestational day 133, we induced UPI, and within an hour of the surgery, injected an equimolar hsiRNA^{sFLT1}-2283/2519 mixture (10 mg/kg each hsiRNA, 20 mg/kg total, n=3). Blood and urine were collected at regular intervals for 4 to 6 weeks (to term) to measure circulating sFLT1 protein, urinary protein levels, and standard blood chemistry markers (Fig 5a). The time points of sample collection vary slightly from animal to animal, due to logistics of working with a free-living baboon colony. Control UPI animals (UPI, n=6) were monitored for 14 days. Sham-operated animals (Controls, n=3) received a non-uterine artery ligation and were also monitored to term.

In hsiRNA^{sFLT1}-2283/2519–treated UPI animals, we observed a potent reduction in circulating sFLT1 protein, as compared to UPI control animals (Fig. 5b), although the kinetics of sFLT1 reduction was somewhat variable. At ~2 weeks post-injection in hsiRNA^{sFLT1}-2283/2519–treated baboons, serum sFLT1 levels were reduced by >50% ($P<0.001$, two-way ANOVA), approaching the levels measured in sham-operated control baboons; these low levels were maintained through to the end of the protocol. Again, similar to sham-operated controls, hsiRNA^{sFLT1}-2283/2519–treated animals had significantly lower blood pressure (Fig 5c) and markedly reduced proteinuria (Fig 5d), consistent with potent reduction of sFLT1. Newborn baboon weights and centiles did not change significantly from controls animal (Supplementary Fig. 9). However, we observed a trend towards lower birth weights in the offspring of baboons treated with hsiRNA^{sFLT1}, likely suggesting a pharmacological effect related to reduction in systemic blood pressure. Additional dose

ranging studies with larger sample sizes will be needed to definitely assess whether the reduction in birth weights are related to sFLT1 repression. Thus, a single injection of hsiRNA^{sFLT1}-2283/2519 potently reduced serum levels of sFLT1 and normalized blood pressure and proteinuria, common clinical manifestations of PE.

To assess clearance of hsiRNA^{sFLT1}-2283 and hsiRNA^{sFLT1}-2519 from blood and their accumulation in tissues, we collected 6 or 7 placenta biopsies and one kidney biopsy from each baboon, in addition to the blood samples noted above. Both hsiRNAs exhibited similar pharmacological behavior, consistent with the expectation that hsiRNA distribution and clearance properties are mainly defined by the oligonucleotide chemical architecture rather than by sequence[20]. The kinetics of hsiRNA clearance from blood were similar in all 3 hsiRNA^{sFLT1}-2283/2519–treated baboons: serum hsiRNA levels remained constant and ranged from 100 to 300 ng/ml during the first hour. By 24 hours, most of the hsiRNA had been cleared from blood, with levels dropping to ~1 ng/ml. Residual hsiRNA levels were detected in blood (<0.1 ng/ml) throughout the study. After day 1, hsiRNA levels in urine remained below 0.5 ng/ml, and fell below the limit of detection after approximately 30 days (Supplementary Fig. 10). Placental hsiRNA levels remained generally constant throughout the four- to six-week study duration (1.6 +/– 0.3 ng/mg for siRNA^{sFLT1}-2283, and 2.6 +/– 0.9 ng/mg for hsiRNA^{sFLT1}-2519; Supplementary Fig. 10). hsiRNA levels in kidney biopsies, collected at day 14, were comparable to placental levels (1.8 +/– 0.9 ng/mg for hsiRNA^{sFLT1}-2283, and 2.7 +/– 1.4 ng/mg for hsiRNA^{sFLT1}-2519). Thus, the 3- to 4-fold difference in hsiRNA accumulation between placenta and kidney that we observed in mice does not hold true in baboons. Moreover, these findings show that persistent low levels of hsiRNA in placenta are sufficient to maintain therapeutic silencing of sFLT1 in this well-accepted non-human primate model of PE.

Discussion

Here we showed that a single dose of hsiRNAs mediating silencing of sFLT1 provided therapeutic benefit in animal models of PE without adverse consequences to the developing fetus. Currently, iatrogenic delivery often occurring preterm remains the only clinically accepted treatment for PE when maternal signs and symptoms become life threatening. Therapeutic strategies aimed at reducing circulating sFLT1 are being pursued as an avenue to treat and prevent severe preeclampsia[2, 47,48,49]. Circulating sFLT1 can be removed from the maternal bloodstream by apheresis, thereby prolonging preeclamptic pregnancy, but this procedure is still in early stage clinical trials[18,19]. Moreover, apheresis is expensive and requires infrastructure that is only available in developed countries.

To validate RNAi-based placental modulation of sFLT1 expression as a therapeutic approach, we chose a baboon model of PE that mimics many features of the human disease, including upregulation of placental sFLT1, a well-validated therapeutic target in PE[43]. Placental growth factor was recently used as a competitive inhibitor of sFLT1 in this baboon model of PE, reducing hypertension and proteinuria with safe progression to birth[50]. Physiological and anatomical similarities between humans and baboons make baboons an appropriate animal model to study PE. Proof-of-concept studies in pregnant baboons therefore represent a key step toward clinical trials in humans[40].

Significant advances in siRNA-based therapeutics, specifically in the area of liver diseases[21,22], recently resulted from two conceptual breakthroughs: (1) extreme chemical stabilization of oligonucleotides [27, 51–53], and (2) optimization of a trimeric GalNAc conjugate that drives selective uptake by hepatocytes[54,55]. Fully chemically modified siRNAs provide unprecedented durability and sustained silencing activity—e.g., up to 9 months duration of effect after a single injection[21, 22]. The hydrophobic cholesterol conjugate supports siRNA delivery to a range of tissues, including liver, kidney, bone marrow, spleen, muscle, and placenta (this study, and[23, 25–27, 35, 36, 56–58]). In mice, cholesterol-conjugated siRNA predominantly accumulates in liver and kidney, but up to seven percent of the injected dose accumulates in placenta. Indeed, the cholesterol moiety was essential for siRNA accumulation in placenta. Although the cholesterol conjugate doesn't provide selective delivery to placenta, delivery to a range of tissues allows functionally-selective silencing when the intended target is a disease gene overexpressed in only one of those tissues. In the case of preeclampsia, sFLT1 is specifically overexpressed in placenta.

sFLT1 represents an exceptional target for siRNA-based therapeutics. Despite significant effort, attempts to develop small molecules and antibodies that selectively downregulate sFLT1 have failed—perhaps not surprising since sFLT1 protein sequences are almost identical to the extracellular domain of full-length FTL1. Recently, a nanoparticle-formulated siRNA that non-selectively targets *sFlt1* and full-length *Flt1,* with ~ 1 mg/kg dose, was found to improve outcomes in a rat model of PE[59]. Nevertheless, rodents do not express the predominant isoform of sFLT1 made in humans, and systemic delivery of therapeutic siRNAs that target full-length *FLT1* could be a liability. Our approach, despite higher dosage, therefore takes advantage of *FLT1* alternative polyadenylation, which creates unique sequence space in *sFLT1* mRNA isoforms that can be selectively targeted by siRNAs.

Our data suggest that a single injection of anti-sFLT1 hsiRNAs might suppress sFLT1 levels for several weeks, potentially extending pregnancy duration. In PE, extension of pregnancy by 2–4 weeks is of clinical significance especially when the disease occurs preterm[1]. The desired level of sFLT1 silencing is only 30% to 40%[18], with a higher degree of silencing being potentially disadvantageous due to reduced uterine blood flow as a consequence of reduced blood pressure[18, 60]. Our data show that a 10 mg/kg dose produces >50% silencing in baboons, so dosing needs to be carefully titrated to tune sFLT1 silencing to the desired level. A strong relationship exists between hsiRNA dosing and the level and duration of target silencing[21].

Interestingly, the initial phases of hsiRNA clearance were distinctly different in baboons and mice. In mice, >99% of hsiRNA was cleared within an hour after injection, but in baboons, hsiRNA blood levels remained constant during the first hour after injection (i.e., around 100 to 200 ng/ml at 15, 30, and 60 min). The rapid clearance of oligonucleotides in rodents compared to non-human primates has been previously reported for other classes of oligonucleotides[61,62], and might reflect the higher metabolic rate of rodents[63]. Careful pharmacological studies are needed to define an optimal chemical composition, clinical dose and schedule to achieve the ideal level and duration of *sFLT1* silencing.

Clinical utility also depends on an acceptable overall toxicity and safety profile. Complete knock-down of sFLT1 in trophoblasts with lentiviral mediated shRNA approach has been associated with decidual hemorrhage[64]. However, at the doses tested (10 to 40 mg/kg), sFlt1 was reduced by 50% which was not associated with adverse effects on blood chemistry, inflammatory markers, or pup viability, weight, vigor and placental vascularization. Importantly, our data indicate that hsiRNAs administered during pregnancy are not transmitted to the fetal tissues other than placenta, minimizing concerns that sFLT1 silencing in the fetus would negatively affect fetal development or pup viability. More detailed safety studies are ongoing.

PE is a disease with a significant unmet medication need in both developed and underdeveloped countries. We show that siRNA-mediated silencing of *sFLT1* mRNAs represents a viable path toward development of a PE therapeutic, particularly when the disease presents preterm. In dry form, siRNA can be stored at ambient temperature for extended periods of time, they are relatively simple to manufacture, and they can be administered by subcutaneous injection. Thus, siRNA therapeutics potentially hold promise to address the needs of preterm PE patients, independent of economic status.

Supplemental Material/Online Methods

hsiRNA design

We designed and synthesized a panel of 47 hsiRNA compounds targeting the human *sFLT1-i13* and *e15a* mRNAs. These sequences span the unique sequence regions and were selected to comply with standard hsiRNA design parameters[31] including assessment of GC content, specificity and low seed compliment frequency[65], elimination of sequences containing miRNA seeds, and examination of thermodynamic bias[34,33] (Supplementary Table 1).

Synthesis of oligonucleotides

Oligonucleotides were synthesized using standard and modified (2′-F, 2′-O-Me) phosphoramidite, solid-phase synthesis conditions using a MerMade 12 (BioAutomation, Irving, Texas) and Expedite DNA/RNA synthesizer (ABI 8909). Unconjugated oligonucleotide strands were grown on controlled pore glass functionalized with a long-chain alkyl amine and Unylinker® terminus (Chemgenes, #N-4000–10) and cholesterol-conjugated oligonucleotides were synthesized on modified solid support (Chemgenes, # N-9166–05). Oligonucleotides were removed from CPG, deprotected, and purified by HPLC as described previously[66]. Purified oligonucleotides were passed over a Hi-Trap cation exchange column to exchange the counter-ion with sodium.

Large scale oligonucleotides were synthesized on an AKTA Oligopilot 100 using standard protocols. Each synthesis was performed at 200umol scale using Unylinker® (ChemGenes, Wilmington, MA) for the antisense strand and a custom solid support containing a cholesterol conjugated CPG for the sense strand. Phosphoramidites were prepared at 0.15M concentrations for both the 2′-O-methyl (ChemGenes, Wilmington, MA) and 2′-fluoro (BioAutomation, Irving, Texas) amidites in ACN. 5-(Benzylthio)-1H-tetrazole was used as the activator at 0.25M. Detritylations were performed using 3% dichloroacetic acid (DCA)

in CH2Cl2. Capping was done with non THF containing reagents CAP A: 20% NMI in CAN and CAP B: 20% Ac2 O, 30% 2,6-lutidine in ACN. Sulfurization was performed with 0.1 M solution of DDTT in ACN for 3 minutes. Phosphoramidite coupling times were 8min for all amidites used. All oligonucleotides were confirmed by HPLC analysis and mass spectrometry.

Cell culture

HeLa and WM-115 cells were purchased from ATCC (ATCC, Manassas, VA; #CCL-2, #CLR-165). HeLa cells were maintained in Dulbecco's Modified Eagle's Medium (Cellgro, Corning, NY; #10–013CV) supplemented with 10% fetal bovine serum (FBS; Gibco, Carlsbad, CA; #26140) and 100 U/ml penicillin/streptomycin (Invitrogen, Carlsbad, CA; #15140) and grown at 37°C and 5% CO_2. Cells were split every 2 to 5 days, and discarded after fifteen passages. WM-115 cells were maintained in Eagle's Minimum Essential Medium medium (Gibco, Carlsbad, CA; #11095) supplemented with 2mM Glutamine, 1% Non Essential Amino Acids, 1% Sodium Pyruvate, 10% % fetal bovine serum (all form Gibco) and 100 U/mL penicillin/streptomycin (Invitrogen) and grown at 37°C and 5% CO_2. Cells were split every 2 to 4 days. CTBs were isolated from human placenta (under IRB protocol number 2009–000317, PI: Karumanchi) and were cultivated as described previously[42,67]. Isolated CTB cells were maintained in M199 medium (Gibco, Carlsbad, CA; #11043023) with 10% FBS.

Direct delivery (passive uptake) of oligonucleotides

For initial hsiRNA library screening cDNA sequences corresponding to unique regions of human *sFLT1 i13* and *e15a* (435 and 567 bp) were cloned into psiCheck-2 vector (Promega, Madison, WI; #C8021) and DualGlo luciferase assay system was used (Promega, Madison, WI; #E2920) according to manufacturer's manual.

Briefly, HeLa cells on 10cm dish were transfected with psiCheck-2-i13 or psiCheck-2-e15a plasmids using Lipofectamin 2000 (Invitrogen, Carlsbad, CA; #11668019) according to manufacturer's manual. 24 hours later cells were plated in DMEM containing 6% FBS at 10,000 cells per well in 96-well cell culture plates. hsiRNA was diluted to twice the final concentration in OptiMEM (Carlsbad, CA; #31985–088), and 50 μL diluted hsiRNA ^{sFLT1} or hsiRNA^{NTC} (NTC- non-targeting control) was added to 50 μL of cells, resulting in 3% FBS final. Cells were incubated for 72 hours at 37°C and 5% CO_2. The primary screen for active hsiRNAs was performed at 1.5 – 3 μM compound, which also served as the maximal dose for *in vitro* dose response assays. To test hsiRNAs in CTB and WM-115 cells, cells were plated at 20,000–30,000 cells per well in 96-well plates in M199 or EMEM media containing 3% FBS and treated with hsiRNAs for 72 hours.

mRNA quantification in cells and tissue punches

mRNA was quantified from both cells and tissue punches using the QuantiGene 2.0 assay kit (Affymetrix, # QS0011) as described previously[68, 69]. Cells were lysed in 250 μL diluted lysis mixture composed of 1 part lysis mixture (Affymetrix, #13228), 2 parts H_2O, and 0.167 μg/μl proteinase K (Affymetrix,# QS0103) for 30 minutes at 55°C. Cell lysates were mixed thoroughly, and 40–80 μl of each lysate was added per well of a capture plate with 20

μl diluted lysis mixture without proteinase K. Probe sets for Human *FLT1, sFLT1-i13, sFLT1-e15a, PPIB and YWHAZ* (Affimetrix; # SA-50494, SA-50495, SA-50496,SA-10003, SA-13271) or mouse *Flt1, sFlt1 and Ppib* (Affimetrix; #SB-50048, SB-50049, SB-10002) were diluted and used according to the manufacturer's recommended protocol. Data sets were normalized to housekeeping gene *Ppib* or *Flt1*.

For analysis of mRNA in mouse tissues, tissue punches (2–5 mg) were homogenized in 300–400 μl of Homogenizing Buffer (Affymetrix, #10642) containing 2 μg/μl proteinase K in 96-well plate format on a QIAGEN TissueLyser II, and 20–60 μl of each lysate was added to a bDNA capture plate. Diluted probe sets were added to each well of the capture plate for a final volume of 100 μL. Signal was amplified according to the Affymetrix protocol. Luminescence was detected on a Veritas Luminometer (Promega, Madison, WI; #998–9100) or Tecan M1000 (Tecan, Morrisville, NC).

Probe sets for Baboon *FLT1, sFLT1-i13, sFLT1-e15a and HPRT* (Affimetrix; #SF-10775, SF-10778, SF-10779, SF-10776) were used for baboon *FLT1* and *sFLT1* mRNA analysis.

Fluorescence imaging—Mice were injected intravenously (tail vein) or subcutaneously (intrascapular) with 10 mg/kg of Cy3-labeled hsiRNA. After 24 hours, mice were sacrificed and tissues were removed, embedded in paraffin, and sliced into 4-μm sections that were mounted on glass slides. Sections were deparaffinized by incubating in Xylene twice for 8 minutes. Sections were rehydrated in serial ethanol dilutions (100%, 95%, and 80%) for 4 minutes each, and then washed twice for 2 minutes with PBS, stained with DAPI. All fluorescent images were acquired with a Leica DMi8 inverted tiling microscope (Leica Microsystems). Images were processed using the Leica software suite (LAS X and LAS X Lite, Leica Microsystems).

ELISA and AST/ALT assays—ELISA for human and mouse sFLT1 was performed according to the manufacturer's instructions (R&D Systems; Quantikine® FLT1, MVR100). All assays were done in duplicate, and the protein levels were calculated using a standard curve derived from known concentrations of the respective recombinant proteins. AST and ALT activities in mouse serum were measured according to the manufacturer's instructions using colorimetric assay kits (Sigma; #MAK055 and #MAK052).

PNA hybridization assay—hsiRNA guide (antisense) strand accumulation in mouse tissues was quantified using a PNA hybridization assay, as described previously[23]. Briefly, tissue punches were homogenized in MasterPure Tissue Lysis Solution (EpiCentre) with added proteinase K (2 mg/mL, Invitrogen) and homogenized using a TissueLyser II (Qiagen), using 100 μL of lysis solution per 10 mg tissue. Following lysis, sodium dodecyl sulfate (SDS) was precipitated with KCl (3 mol/l) and cleared supernatant was hybridized to a Cy3-labeled PNA oligonucleotide fully complementary to the guide strand (PNABio). This mixture was analyzed by high-performance liquid chromatography (HPLC). Cy3-labeled peaks were integrated and plotted on an internal calibration curve. Mobile phase for HPLC was 50% water, 50% acetonitrile, 25 mmol/l Tris-HCl (pH 8.5) and 1 mmol/l ethylenediamine-tetraacetate. The salt gradient was 0–800 mmol/l $NaClO_4$.

Animals, efficacy, and safety—Wild-type mice C57BL/6J or pregnant CD1 were purchased from Jackson Laboratory (Bar Harbor, ME). All animal procedures were approved by the University of Massachusetts Medical School Institutional care and use of animals committee (IACUC, protocol number A-2411) or at the Beth Israel Deaconess Medical Center (IACUC, protocol number 048–2017). Mice were 6- to 10-weeks old at the time of experiments. All animals were kept on a 12-hour light/dark cycle in a pathogen-free facility, with food and water provided *ad libitum*..

Four 2.0 mm punches per side were made, three processed individually for the Quantigene 2.0 Assay (Affymetrix, #QS0011). For systemic administration of hsiRNA^{sFLT1}, mice were injected with either phosphate buffered saline (PBS) or with different amounts of hsiRNA^{sFLT1} or hsiRNA^{NTC} resuspended in PBS, either through the tail vein or subcutaneously at the nape of the neck (interscapular). After treatment mice were deeply anesthetized with 0.1% Avertin, and after cervical dislocation, tissues were collected and processed immediately or stored in RNAlater (Sigma, #R0901) for later use.

5’-RACE-PCR analysis—Total RNA was isolated from placentas from mice treated with of hsiRNA ^{sFLT1}, hsiRNA^{NTC} (2×20 mg/kg, IV) and PBS as described above, using TRIzol reagent (Life Technologies). 5 μg of isolated RNA was used for 5’-RACE analysis using GeneRacer kit (Life Technologies) without initial pretreatment as described before[24]. Total RNA samples were ligated to GeneRacer RNA adaptor and ligated RNA was used for reverse transcription using gene-specific primer (GSP1: 5’-GCGTCCCAGGTTGCTGCTATGAAGCAGAA −3’). cDNA was amplified by PCR using GSP1 and GeneRacer 5’-primer (5’-CGACTGGAGCACGAGGACACTGA-3’). Amplified PCR products were resolved and visualized on agarose gel with ethidium bromide. Final PCR products were cloned onto pCR 4-TOPO vector (Invitrogen) and specific cleavage site was confirmed by sequencing.

Immunohistochemistry—Paraffin sections (2 μm) of placental tissue were deparaffinized and rehydrated. Optimal staining was achieved with an antigen retrieval method that was performed in 10 mmol/l citric acid, pH 6.00 for 15 min. Endogenous peroxidase was quenched with 3% H_2O_2 in ddH_2O for 15 min. Sections were blocked with 2.5% normal horse serum at room temperature for 40 min and incubated 40 min with 1:50 dilution of primary CD31 antibody (BCAM, Cambridge, MA). Specific labeling was detected with an ImmPRESS HRP Anti-Rabbit IgG (Peroxidase) Polymer Detection Kit (Vector Laboratories, Burlingame, CA). The enzymatic reaction product was achieved by using VECTOR NovaRED Peroxidase (HRP) substrate to give a red- brown precipitate, and the sections were counterstained with hematoxylin, dehydrated, and mounted in Permount (Thermo Fisher Scientific, Atlanta, GA). Sections with no primary antibody were used as negative control slides.

Non-Human Primate Model of Preeclampsia—These experiments were approved by the Sydney Local Health District Animal Welfare Committee. We used a well-established baboon uterine artery ischemia model of preeclampsia that has been described previously[43]. This model is characterized by rapid rise in plasma sFLT1 levels that correlate with the onset of hypertension following placental ischemia[43]. Female pregnant baboons (*Papio*

hamadryas) from the National Baboon Colony, New South Wales, Australia were provided food and water *ad libitum*. At the beginning of the protocol the animals were 127 days of gestation of a normally 182 day gestation. Animals were anesthetized using ketamine infusion (0.2mg/kg/min) with a premedication of metoclopramide (5mg intramuscularly as well as clonazepam (intravenously at 0.01mg/kg for seizure prophylaxis). All animals received procedural antibiotics benzylpenicillin and gentamicin intravenously at the time of surgery. They also received buprenorphine (0.02mg/kg, intramuscularly) for analgesia, before, immediately after, 8 and 16 hrs after the procedure. Pain was scored and further analgesia could be administered but was not required. All animals were acclimatised for several days and then a radiotelemeter was surgically inserted into a branch of the femoral artery and passed into the aorta to about the level of the renal arteries, to monitor intra-arterial blood pressure (PA-D70, DataSci, Minnesota, USA) as has been described previously[13]. After 1 week, to allow for recovery, uteroplacental ischemia (UPI) was induced experimentally. Briefly, animals underwent non-dominant unilateral uterine artery complete ligation through a midline abdominal transperitoneal incision. The iliac vessels were visualised and the uterine artery identified at its point of origin from the internal iliac artery. The uterine artery was dissected and irrigated with 1% lidocaine solution to reduce arterial spasm. The vessel was then ligated with 4.0 silk sutures. Complete ligation was verified by performing repeat uterine artery duplex ultrasonography after the procedure that demonstrated no-flow in the artery where previously flow had been demonstrated. The peritoneum, muscle and skin were closed in layers. Post-surgery, blood and urine samples were collected as well as a chorionic villous sample (CVS) performed on around days 3, 6, 10 and 14 of UPI. The exact time of blood collection is shown at figures. The variability in exact time of blood collection is due to logistical complications of working with free-living baboon colony. hsiRNA^{sFLT1} (equimolar mixture of hsiRNA^{sFLT1}-2283 and hsiRNA^{sFLT1}-2519 (20 mg/kg total) was injected intravenously within an hour of UPI procedure. A timeline demonstrates when the procedures were performed (**Fig.5a**). Renal biopsies were done as previously described[50]. All animals were allowed to deliver spontaneously (natural labor) and fetal weights measured at birth with the exception of animal #3 (that received hsiRNA therapy) which underwent emergent C-section for unrelated condition (acute chorioamnionitis confirmed by histology) at gestational day 163 and then euthanized. Data for controls were derived from sham surgery animals as described previously[13].

Statistical analysis—Data were analyzed using GraphPad Prism 7 software (GraphPad Software, Inc., San Diego, CA). Concentration-dependent IC50 curves were fitted using a log(inhibitor) vs. response – variable slope (four parameters). The lower limit of the curve was set at zero, and the upper limit of the curve was set at 100. For each independent mouse experiment, the level of knockdown at each dose was normalized to the mean of the control group (PBS or untreated groups). *In vivo* data were analyzed using a Kruskal-Wallis one-way ANOVA with Dunn's post-hoc analysis or two way ANOVA (time course of sFlt1 serum concentration) as appropriate for experimental design. Differences in all comparisons were considered significant at P values less than 0.05.

Supplementary Material

Refer to Web version on PubMed Central for supplementary material.

Acknowledgments

This project was funded by the National Institutes of Health (R01 HD086111 and S10 OD020012) and the Bill and Melinda Gates Foundation (OPP1086170). We especially thank Darryl Conte for help revising the manuscript, and the Khvorova Lab for their support.

REFERENCES

1. Stevens W et al. Short-term costs of preeclampsia to the United States health care system. American journal of obstetrics and gynecology 217, 237–248 e216 (2017). [PubMed: 28708975]
2. Maynard SE et al. Excess placental soluble fms-like tyrosine kinase 1 (sFlt1) may contribute to endothelial dysfunction, hypertension, and proteinuria in preeclampsia. The Journal of clinical investigation 111, 649–658 (2003). [PubMed: 12618519]
3. Levine RJ et al. Circulating angiogenic factors and the risk of preeclampsia. The New England journal of medicine 350, 672–683 (2004). [PubMed: 14764923]
4. Heydarian M et al. Novel splice variants of sFlt1 are upregulated in preeclampsia. Placenta 30, 250–255 (2009). [PubMed: 19147226]
5. Young BC, Levine RJ & Karumanchi SA Pathogenesis of preeclampsia. Annual review of pathology 5, 173–192 (2010).
6. Aubuchon M, Schulz LC & Schust DJ Preeclampsia: animal models for a human cure. Proceedings of the National Academy of Sciences of the United States of America 108, 1197–1198 (2011). [PubMed: 21233419]
7. Chaiworapongsa T et al. Evidence supporting a role for blockade of the vascular endothelial growth factor system in the pathophysiology of preeclampsia. Young Investigator Award. *American journal of obstetrics and gynecology* 190, 1541–1547; discussion 1547–1550 (2004). [PubMed: 15284729]
8. Lu F et al. The effect of over-expression of sFlt-1 on blood pressure and the occurrence of other manifestations of preeclampsia in unrestrained conscious pregnant mice. American journal of obstetrics and gynecology 196, 396 e391–397; discussion 396 e397 (2007).
9. Ahmad S & Ahmed A Elevated placental soluble vascular endothelial growth factor receptor-1 inhibits angiogenesis in preeclampsia. Circ Res 95, 884–891 (2004). [PubMed: 15472115]
10. Redman CW & Sargent IL Latest advances in understanding preeclampsia. Science 308, 1592–1594 (2005). [PubMed: 15947178]
11. Vorlova S et al. Induction of antagonistic soluble decoy receptor tyrosine kinases by intronic polyA activation. Molecular cell 43, 927–939 (2011). [PubMed: 21925381]
12. Kendall RL & Thomas KA Inhibition of vascular endothelial cell growth factor activity by an endogenously encoded soluble receptor. Proceedings of the National Academy of Sciences of the United States of America 90, 10705–10709 (1993). [PubMed: 8248162]
13. Bujold E et al. Evidence supporting that the excess of the sVEGFR-1 concentration in maternal plasma in preeclampsia has a uterine origin. The journal of maternal-fetal & neonatal medicine : the official journal of the European Association of Perinatal Medicine, the Federation of Asia and Oceania Perinatal Societies, the International Society of Perinatal Obstet 18, 9–16 (2005).
14. Zeisler H et al. Predictive Value of the sFlt-1:PlGF Ratio in Women with Suspected Preeclampsia. The New England journal of medicine 374, 13–22 (2016). [PubMed: 26735990]
15. Sunderji S et al. Automated assays for sVEGF R1 and PlGF as an aid in the diagnosis of preterm preeclampsia: a prospective clinical study. American journal of obstetrics and gynecology 202, 40 e41–47 (2010).
16. Rana S et al. Angiogenic factors and the risk of adverse outcomes in women with suspected preeclampsia. Circulation 125, 911–919 (2012). [PubMed: 22261192]
17. Chaiworapongsa T et al. Plasma concentrations of angiogenic/anti-angiogenic factors have prognostic value in women presenting with suspected preeclampsia to the obstetrical triage area: a

prospective study. The journal of maternal-fetal & neonatal medicine : the official journal of the European Association of Perinatal Medicine, the Federation of Asia and Oceania Perinatal Societies, the International Society of Perinatal Obstet 27, 132–144 (2014).

18. Thadhani R et al. Pilot study of extracorporeal removal of soluble fms-like tyrosine kinase 1 in preeclampsia. Circulation 124, 940–950 (2011). [PubMed: 21810665]
19. Thadhani R et al. Removal of Soluble Fms-Like Tyrosine Kinase-1 by Dextran Sulfate Apheresis in Preeclampsia. J Am Soc Nephrol 27, 903–913 (2016). [PubMed: 26405111]
20. Khvorova A & Watts JK The chemical evolution of oligonucleotide therapies of clinical utility. Nature biotechnology 35, 238–248 (2017).
21. Fitzgerald K et al. A Highly Durable RNAi Therapeutic Inhibitor of PCSK9. The New England journal of medicine 376, 41–51 (2017). [PubMed: 27959715]
22. Khvorova A Oligonucleotide Therapeutics - A New Class of Cholesterol-Lowering Drugs. The New England journal of medicine 376, 4–7 (2017). [PubMed: 28052224]
23. Haraszti RA et al. 5-Vinylphosphonate improves tissue accumulation and efficacy of conjugated siRNAs in vivo. Nucleic acids research 45, 7581–7592 (2017). [PubMed: 28591791]
24. Soutschek J et al. Therapeutic silencing of an endogenous gene by systemic administration of modified siRNAs. Nature 432, 173–178 (2004). [PubMed: 15538359]
25. Byrne M et al. Novel hydrophobically modified asymmetric RNAi compounds (sd-rxRNA) demonstrate robust efficacy in the eye. Journal of ocular pharmacology and therapeutics : the official journal of the Association for Ocular Pharmacology and Therapeutics 29, 855–864 (2013).
26. Khan T et al. Silencing Myostatin Using Cholesterol-conjugated siRNAs Induces Muscle Growth. Molecular Therapy - Nucleic Acids 5 (2016).
27. Hassler MR et al. Comparison of partially and fully chemically-modified siRNA in conjugate-mediated delivery in vivo. Nucleic acids research 46, 2185–2196 (2018). [PubMed: 29432571]
28. Ashar-Patel A et al. FLT1 and transcriptome-wide polyadenylation site (PAS) analysis in preeclampsia. Sci Rep 7, 12139 (2017). [PubMed: 28939845]
29. Palmer KR et al. Placental-Specific sFLT-1 e15a Protein Is Increased in Preeclampsia, Antagonizes Vascular Endothelial Growth Factor Signaling, and Has Antiangiogenic Activity. Hypertension 66, 1251–1259 (2015). [PubMed: 26416849]
30. Souders CA et al. Circulating Levels of sFlt1 Splice Variants as Predictive Markers for the Development of Preeclampsia. Int J Mol Sci 16, 12436–12453 (2015). [PubMed: 26042465]
31. Birmingham A et al. A protocol for designing siRNAs with high functionality and specificity. Nat Protoc 2, 2068–2078 (2007). [PubMed: 17853862]
32. Anderson EM et al. Experimental validation of the importance of seed complement frequency to siRNA specificity. Rna 14, 853–861 (2008). [PubMed: 18367722]
33. Khvorova A, Reynolds A & Jayasena SD Functional siRNAs and miRNAs exhibit strand bias. Cell 115, 209–216 (2003). [PubMed: 14567918]
34. Schwarz DS et al. Asymmetry in the assembly of the RNAi enzyme complex. Cell 115, 199–208 (2003). [PubMed: 14567917]
35. Alterman JF et al. Hydrophobically Modified siRNAs Silence Huntingtin mRNA in Primary Neurons and Mouse Brain. Mol Ther Nucleic Acids 4, e266 (2015). [PubMed: 26623938]
36. Godinho B et al. Pharmacokinetic Profiling of Conjugated Therapeutic Oligonucleotides: A High-Throughput Method Based Upon Serial Blood Microsampling Coupled to Peptide Nucleic Acid Hybridization Assay. Nucleic Acid Ther (2017).
37. Ly S et al. Visualization of self-delivering hydrophobically modified siRNA cellular internalization. Nucleic acids research 45, 15–25 (2017). [PubMed: 27899655]
38. Wang S et al. Cellular uptake mediated by epidermal growth factor receptor facilitates the intracellular activity of phosphorothioate-modified antisense oligonucleotides. Nucleic acids research (2018).
39. Allerson CR et al. Fully 2'-modified oligonucleotide duplexes with improved in vitro potency and stability compared to unmodified small interfering RNA. J Med Chem 48, 901–904 (2005). [PubMed: 15715458]

40. Sela S et al. A novel human-specific soluble vascular endothelial growth factor receptor 1: cell-type-specific splicing and implications to vascular endothelial growth factor homeostasis and preeclampsia. Circ Res 102, 1566–1574 (2008). [PubMed: 18515749]
41. Holme AM, Roland MC, Henriksen T & Michelsen TM In vivo uteroplacental release of placental growth factor and soluble Fms-like tyrosine kinase-1 in normal and preeclamptic pregnancies. American journal of obstetrics and gynecology 215, 782 e781–782 e789 (2016).
42. Rajakumar A et al. Transcriptionally active syncytial aggregates in the maternal circulation may contribute to circulating soluble fms-like tyrosine kinase 1 in preeclampsia. Hypertension 59, 256–264 (2012). [PubMed: 22215706]
43. Makris A et al. Uteroplacental ischemia results in proteinuric hypertension and elevated sFLT-1. Kidney international 71, 977–984 (2007). [PubMed: 17377512]
44. Amadio M, Govoni S & Pascale A Targeting VEGF in eye neovascularization: What's new?: A comprehensive review on current therapies and oligonucleotide-based interventions under development. Pharmacol Res 103, 253–269 (2016). [PubMed: 26678602]
45. Ambati BK et al. Corneal avascularity is due to soluble VEGF receptor-1. Nature 443, 993–997 (2006). [PubMed: 17051153]
46. Lertkiatmongkol P, Liao D, Mei H, Hu Y & Newman PJ Endothelial functions of platelet/endothelial cell adhesion molecule-1 (CD31). Curr Opin Hematol 23, 253–259 (2016). [PubMed: 27055047]
47. Karumanchi SA Angiogenic Factors in Preeclampsia: From Diagnosis to Therapy. Hypertension 67, 1072–1079 (2016). [PubMed: 27067718]
48. Bergmann A et al. Reduction of circulating soluble Flt-1 alleviates preeclampsia-like symptoms in a mouse model. J Cell Mol Med 14, 1857–1867 (2010). [PubMed: 19538465]
49. Spradley FT et al. Placental Growth Factor Administration Abolishes Placental Ischemia-Induced Hypertension. Hypertension 67, 740–747 (2016). [PubMed: 26831193]
50. Makris A et al. Placental Growth Factor Reduces Blood Pressure in a Uteroplacental Ischemia Model of Preeclampsia in Nonhuman Primates. Hypertension 67, 1263–1272 (2016). [PubMed: 27091894]
51. Yu D et al. Single-stranded RNAs use RNAi to potently and allele-selectively inhibit mutant huntingtin expression. Cell 150, 895–908 (2012). [PubMed: 22939619]
52. Nair JK et al. Impact of enhanced metabolic stability on pharmacokinetics and pharmacodynamics of GalNAc-siRNA conjugates. Nucleic acids research 45, 10969–10977 (2017). [PubMed: 28981809]
53. Pasi KJ et al. Targeting of Antithrombin in Hemophilia A or B with RNAi Therapy. The New England journal of medicine 377, 819–828 (2017). [PubMed: 28691885]
54. Matsuda S et al. siRNA conjugates carrying sequentially assembled trivalent N-acetylgalactosamine linked through nucleosides elicit robust gene silencing in vivo in hepatocytes. ACS Chem Biol 10, 1181–1187 (2015). [PubMed: 25730476]
55. Nair JK et al. Multivalent N-acetylgalactosamine-conjugated siRNA localizes in hepatocytes and elicits robust RNAi-mediated gene silencing. J Am Chem Soc 136, 16958–16961 (2014). [PubMed: 25434769]
56. Wolfrum C et al. Mechanisms and optimization of in vivo delivery of lipophilic siRNAs. Nature biotechnology 25, 1149–1157 (2007).
57. Krutzfeldt J et al. Silencing of microRNAs in vivo with 'antagomirs'. Nature 438, 685–689 (2005). [PubMed: 16258535]
58. Baerlocher GM, Burington B & Snyder DS Telomerase Inhibitor Imetelstat in Essential Thrombocythemia and Myelofibrosis. The New England journal of medicine 373, 2580 (2015).
59. Yu J, Jia J, Guo X, Chen R & Feng L Modulating circulating sFlt1 in an animal model of preeclampsia using PAMAM nanoparticles for siRNA delivery. Placenta 58, 1–8 (2017). [PubMed: 28962687]
60. Khankin EV, Mandala M, Colton I, Karumanchi SA & Osol G Hemodynamic, vascular, and reproductive impact of FMS-like tyrosine kinase 1 (FLT1) blockade on the uteroplacental circulation during normal mouse pregnancy. Biology of reproduction 86, 57 (2012). [PubMed: 22075472]

61. Yu RZ et al. Cross-species pharmacokinetic comparison from mouse to man of a second-generation antisense oligonucleotide, ISIS 301012, targeting human apolipoprotein B-100. Drug Metab Dispos 35, 460–468 (2007). [PubMed: 17172312]

62. Geary RS, Norris D, Yu R & Bennett CF Pharmacokinetics, biodistribution and cell uptake of antisense oligonucleotides. Advanced Drug Delivery Reviews 87, 46–51 (2015). [PubMed: 25666165]

63. Savage VM et al. Scaling of number, size, and metabolic rate of cells with body size in mammals. Proceedings of the National Academy of Sciences of the United States of America 104, 4718–4723 (2007). [PubMed: 17360590]

64. Fan X et al. Endometrial VEGF induces placental sFLT1 and leads to pregnancy complications. The Journal of clinical investigation 124, 4941–4952 (2014). [PubMed: 25329693]

65. Anderson E, Boese Q, Khvorova A & Karpilow J Identifying siRNA-induced off-targets by microarray analysis. Methods in molecular biology 442, 45–63 (2008). [PubMed: 18369777]

66. Osborn MF et al. Guanabenz (Wytensin) selectively enhances uptake and efficacy of hydrophobically modified siRNAs. Nucleic acids research 43, 8664–8672 (2015). [PubMed: 26400165]

67. Rajakumar A et al. Novel soluble Flt-1 isoforms in plasma and cultured placental explants from normotensive pregnant and preeclamptic women. Placenta 30, 25–34 (2009). [PubMed: 19010535]

68. Coles AH et al. A High-Throughput Method for Direct Detection of Therapeutic Oligonucleotide-Induced Gene Silencing In Vivo. Nucleic Acid Ther 26, 86–92 (2016). [PubMed: 26595721]

69. Nikan M et al. Docosahexaenoic Acid Conjugation Enhances Distribution and Safety of siRNA upon Local Administration in Mouse Brain. Mol Ther Nucleic Acids 5, e344 (2016). [PubMed: 27504598]

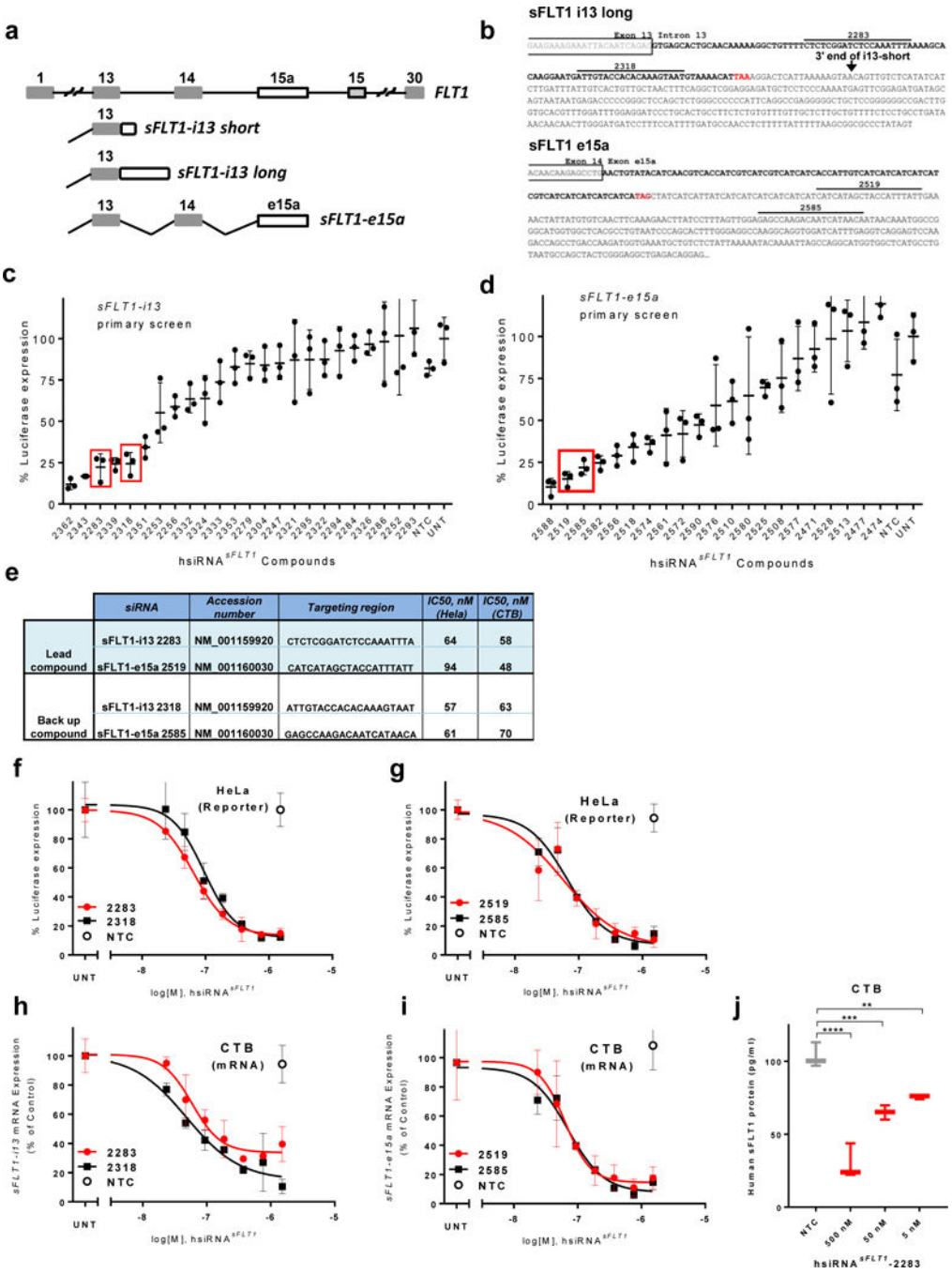

	siRNA	Accession number	Targeting region	IC50, nM (Hela)	IC50, nM (CTB)
Lead compound	sFLT1-i13 2283	NM_001159920	CTCTCGGATCTCCAAATTTA	64	58
	sFLT1-e15a 2519	NM_001160030	CATCATAGCTACCATTTATT	94	48
Back up compound	sFLT1-i13 2318	NM_001159920	ATTGTACCACACAAAGTAAT	57	63
	sFLT1-e15a 2585	NM_001160030	GAGCCAAGACAATCATAACA	61	70

Figure 1. Development of hydrophobically modified, chemically stabilized hsiRNA compounds against sFLT1.

a. Schematic representation of exon-intron structure of *sFLT1-i13* and *sFLT1-e15a* mRNAs. **b.** *sFLT1-i13* and *sFLT1-e15a* unique sequence regions. Locations of lead siRNA target sites are indicated. Stop codons are shown in red. **c-d**. Results of screen for hsiRNAs (1.5 μM) that silence *sFLT1-i13* and *sFLT1-e15a* using luciferase-based reporters in HeLa cells. siRNA numbers correspond to the 5' position of the siRNA target site in the mRNA. UNT, untreated control, NTC, non-targeting control. (n=3, mean ± SD). Solid bars indicate lead

compounds selected for further evaluation. **e**. siRNAs targeting *sFLT1-i13* and *sFLT1-e15a*. **f-g.** Dose-response curves of lead hsiRNA^{sFLT1} silencing of *sFLT1-i13* and *sFLT1-e15a* luciferase reporters in HeLa cells. **h-i.** Dose-response curves of lead hsiRNA^{sFLT1} silencing of *sFLT1-i13* and *sFLT1-e15a* mRNAs in cytotrophoblast (CTB) cells. (n=3, mean ± SD). **j**. sFlt1 protein levels produced by CTB cells treated with hsiRNA^{sFLT1}-2283 or hsiRNA^{NTC}. Level of sFlt1 protein was measured by ELISA (n=2, mean ± SD) (** $P<0.01$, * $P,<0.05$, *ns* - not significant, one-way ANOVA).

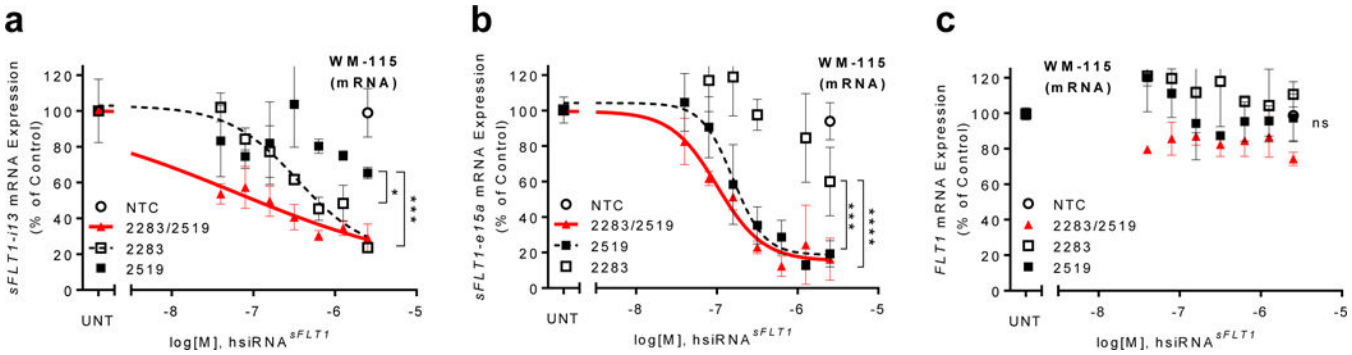

Figure 2. Efficient silencing of sFLT1 by hsiRNA^{sFLT1}-2283/2519 mixture *in vitro*.

a-c. Dose-response silencing of *sFLT1-i13*, *sFLT1-e15a*, or *Flt1* mRNAs respectively, by individual hsiRNAs or the equimolar hsiRNA^{sFLT1}-2283/2519 mixture in WM-115 cells. mRNA levels were measured using QuantiGene® 2 (Affymetrix) and normalized to the housekeeping gene *FLT1* (n=3, mean ± SD). *NTC* - non-targeting control (**** *P<0.0001*, *** *P<0.001*, * *P<0.05*, *ns* - not significant; two-way ANOVA).

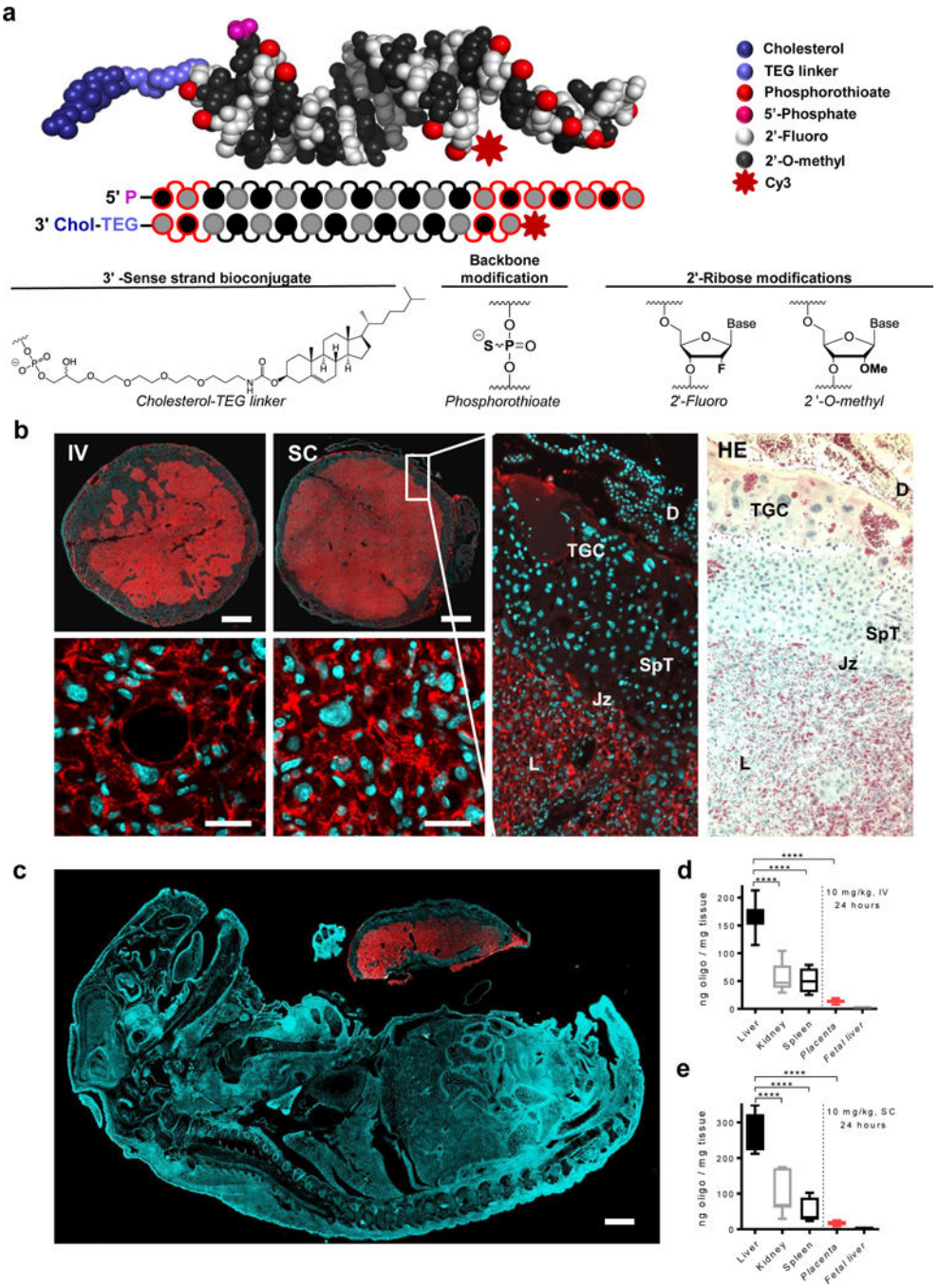

Figure 3. Full chemical stabilization of cholesterol-conjugated hsiRNAs enables systemic delivery to placental labyrinth.

a. Structure and chemical composition of fully chemically-stabilized cholesterol-conjugated siRNAs (hsiRNA). **b**. Distribution of Cy3-hsiRNA^{sFLT1}-2283 (red) in placentas of mice following intravenous (IV) or subcutaneous (SC) injection. Nuclei were stained with DAPI (blue). Matched slides were stained with hematoxylin and eosin (***HE***). Scale bars, 1 mm (upper panels), 25 μm (lower panels). **c**. Distribution of Cy3-labeled hsiRNA^{sFLT1}-2283 (red) in mouse fetus. Nuclei were stained with DAPI (blue). Representative image of two

experiments in which the dam received an IV injection of Cy3-labeled hsiRNA^{sFLT1}-2283. **d-e**. Bar graphs of hsiRNA^{sFLT1}-2283 levels in indicated tissues of mice from ***b***. Guide strand levels were measure using the PNA hybridization assay. (n=3, mean ± SD). *TGC*, Trophoblast Giant Cells; *SpT*, Spongio Trophoblast; *L*, Labyrinth; *Jz*, Junctional zone; *D*, Decidua. (**** *P<0.0001*; one-way ANOVA).

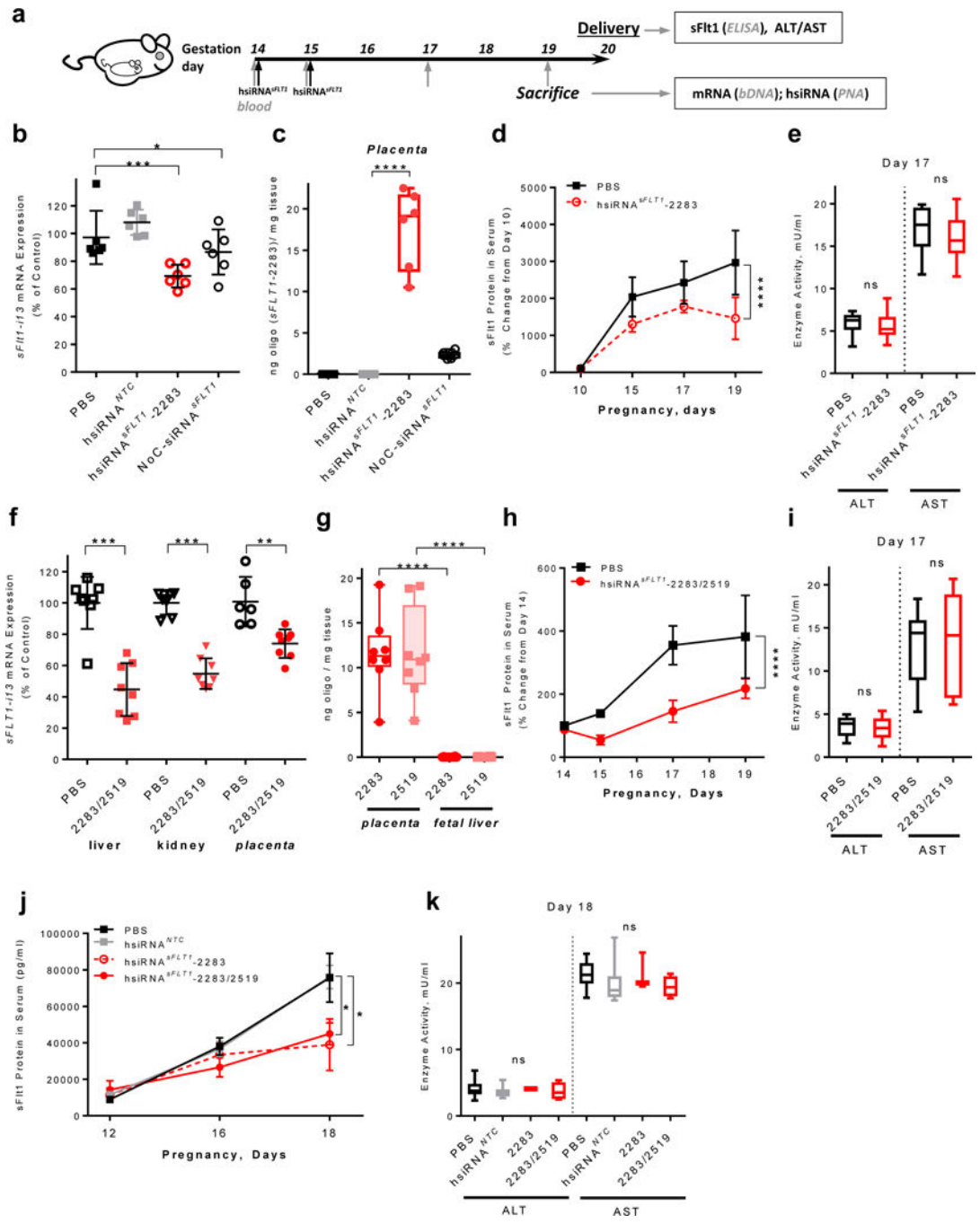

Figure 4. Efficient silencing of *sFLT1* mRNA and protein by hsiRNA^{sFLT1} in pregnant mice.

a.Experimental design for *in vivo* testing of siRNA. Pregnant CD1 mice were injected with 20 mg/kg of hsiRNA^{sFLT1} (IV, tail vein) on days E14 and E15, and sacrificed on day E19 or allowed to deliver pups on day E20. Blood was collected on the indicated days (gray vertical arrows). Samples were prepared at the end points for the indicated assays. **b.** *sFLT1-i13* mRNA levels in placentas of mice treated with PBS, hsiRNA^{NTC}, hsiRNA^{sFLT1}, or NoC-siRNA^{sFLT1}. mRNAs were measured QuantiGene® 2 (Affymetrix) and levels were normalized to housekeeping gene (*mFlt1*), and presented as percent of PBS control (n=6,

mean ± SD). **c.** Amount of hsiRNA accumulated in indicated tissues five days after first injection of mice from ***b***. Measured by PNA hybridization assay. **d.** sFlt1 protein levels measured by ELISA (n=9, mean ± SD). **e.** ALT/AST enzymes activities at day E17 in mice injected with PBS or hsiRNA^{sFLT1} from ***d***. **f**. *sFLT1-i13* mRNA levels in liver, kidney, or placenta of CD1 mice injected (IV, tail vein) on day E14 and E15 with equimolar hsiRNA^{sFLT1}-2283/2519 mixture and sacrificed at E19. mRNA levels were measured QuantiGene® 2 (Affymetrix), normalized to *Flt1*, and presented as percent of PBS control (n=8, mean ± SD). **g.** Amount of hsiRNA accumulated in fetal tissues (placenta and liver) from mice from ***f***, five days after injection. Measured by PNA hybridization assay. **h**. sFlt1 protein levels from mice injected with hsiRNA^{sFLT1}-2283/2519 measured by ELISA (n=8, mean ± SD). **i.** ALT/AST enzyme activities on day E17 in mice injected with equimolar hsiRNA^{sFLT1}-2283/2519 mixture from ***h***. **j.** sFlt1 protein levels from mice injected with PBS, hsiRNA^{NTC}, hsiRNA^{sFLT1}-2283 and hsiRNA^{sFLT1}-2283/2519 (2× 20 mg/kg) measured by ELISA (n=10 for PBS and NTC, n=4 for hsiRNA^{sFLT1}; mean ± SEM). **k.** ALT/AST enzyme activities on day E18 in mice injected in ***j***. (**** *P<0.0001*, *** *P<0.001*, ** *P<0.01*, * *P<0.05*, *ns* - not significant; one-way ANOVA for ***b***, ***c***, ***e***, ***f***, ***g***, ***i*** and ***k***; two-way ANOVA for ***d***, ***h*** and ***j***).

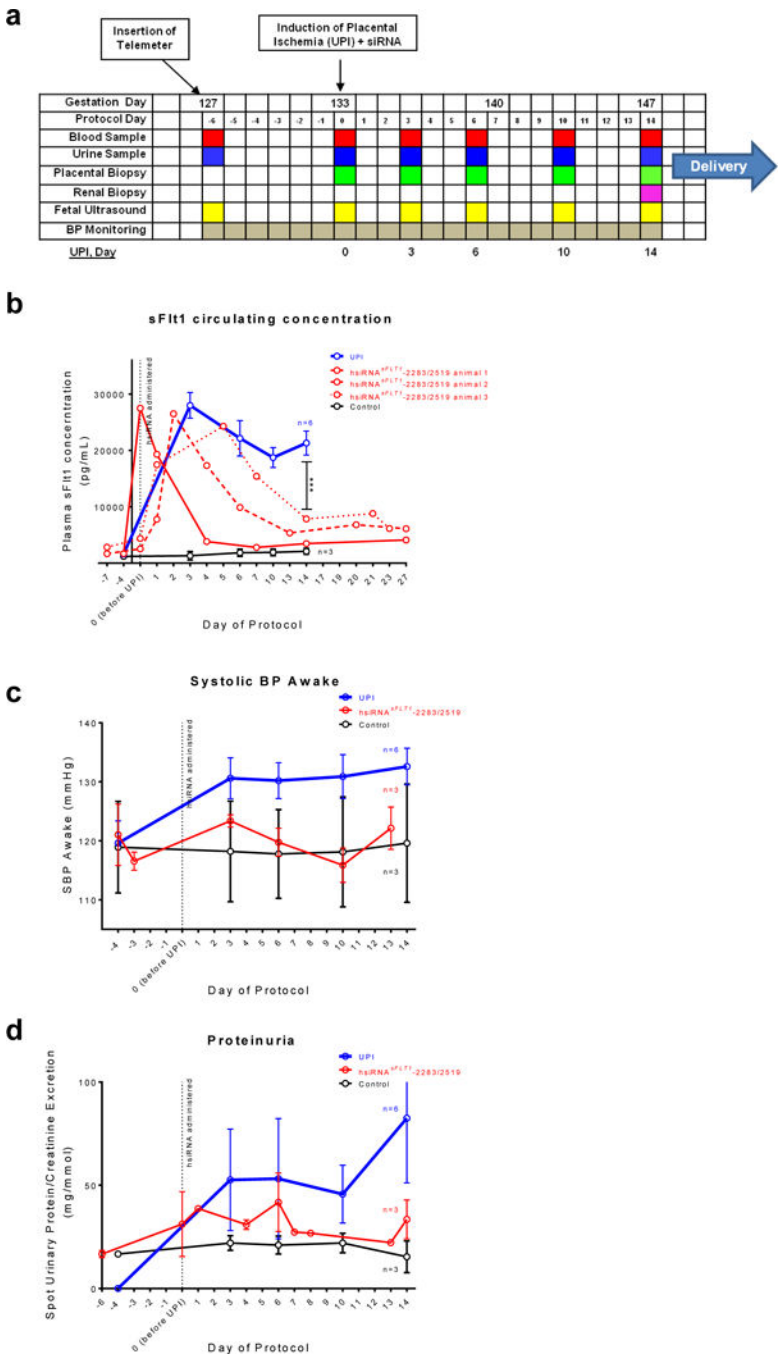

Figure 5. hsiRNA^{sFLT1}-2283/2519 treatment lowers sFLT1 serum levels and normalize blood pressure and proteinuria in NHP model of PE.

a. The timeline for uteroplacental ischemia induction (UPI) model of PE in pregnant baboon. Data collected for hsiRNA^{sFLT1}-2283/2519-treated UPI animals (n=3, mean ±SEM), PBS treated UPI animals (n=6, mean ±SEM), and controls (sham surgery, no UPI) (n=3, mean ±SEM) (***$P<0.001$, two-way ANOVA; UPI *vs* hsiRNA^{sFLT1}). **b.** sFLT1 serum concentration measured by ELISA **c.** Systolic blood pressure (BP, awake) plotted from telemetry recordings. **d.** Proteinuria presented as spot protein/creatinine ratio.